Konrad-Zuse-Zentrum
für Informationstechnik Berlin

Takustraße 7
D-14195 Berlin-Dahlem
Germany

P. DEUFLHARD B. ERDMANN R. ROITZSCH G.T. LINES

Adaptive Finite Element Simulation of Ventricular Fibrillation Dynamics

ZIB-Report 06–49 (November 2006)

Adaptive Finite Element Simulation of Ventricular Fibrillation Dynamics[1]

Peter Deuflhard[2,4] Bodo Erdmann[2] Rainer Roitzsch[2] Glenn Terje Lines[3]

Abstract

The dynamics of ventricular fibrillation caused by irregular excitation is simulated in the frame of the monodomain model with an action potential model due to Aliev-Panfilov for a human 3D geometry. The numerical solution of this multiscale reaction-diffusion problem is attacked by algorithms which are fully adaptive in both space and time (code library KARDOS). The obtained results clearly demonstrate an accurate resolution of the cardiac potential during the excitation and the plateau phases (in the regular cycle) as well as after a reentrant excitation (in the irregular cycle).

Keywords: reaction-diffusion equations, Aliev-Panfilov model, electrocardiology, adaptive finite elements, adaptive Rothe method

[1]Supported by the DFG Research Center MATHEON "Mathematics for key technologies" in Berlin.

[2]Zuse Institute Berlin, Takustr. 7, 14195 Berlin-Dahlem, Germany. E-mail: {deuflhard, erdmann, roitzsch}@zib.de

[3]Simula Research Laboratory, P.O. Box 134, N-1325 Lysaker, Norway. E-mail: glennli@simula.no

[4]Freie Universität Berlin, Dept. of Mathematics and Computer Science, Arnimallee 6, 14159 Berlin-Dahlem, Germany.

Contents

Introduction

Recent advances in cardiac electrophysiology are progressively revealing the extremely complex multiscale structure of the bioelectrical activity of the heart, from the microscopic activity of ion channels of the cellular membrane to the macroscopic properties of the anisotropic propagation of excitation and recovery fronts in the whole heart. Mathematical models of these phenomena have reached a degree of sophistication that makes them a real challenge for numerical simulation. A detailed introduction can be found in the recent monograph of Sundnes et al. [11]. In 1996, Aliev and Panfilov [3] suggested a still quite simple model for an adequate description of the dynamics of pulse propagation in cardiac tissue as it occurs in cardiac arrhythmia like atrial or ventricular fibrillation. The present paper will focus on this model.

The recent paper [4] by Colli Franzone et al. had already presented a simulation of the evolution of a full regular heartbeat, from the excitation (depolarization) phase to the plateau and recovery (repolarization) phases. However, even though that paper had successfully tested the fully adaptive 3D code KARDOS due to Lang [6, 5, 2], which took correct care of the multiscale nature of the models, it had only been applied to a simple 3D quadrilateral instead of a realistic heart geometry. As a follow-up, the present paper will perform the necessary step towards a realistic 3D human heart geometry (visible human) and, at the same time, include the study of effects caused by an irregular out of phase stimulus leading to fibrillation.

The paper is organized as follows. First, in Section 1, we briefly sketch different cardiac models including the Aliev-Panfilov model. Then, in Section 2, we present the results of several simulations on the full heart geometry for the Aliev-Panfilov model. Special attention is paid to the gain caused by adaptivity of the algorithm. Throughout the paper, visualizations have been made using the software environment Amira [1, 10].

1 Cardiac models

There exists a large variety of cardiac models with different depth of details to be captured. In this section, we briefly sketch the main ones. For more details we refer to the book Sundnes et al. [11] or to our recent article Colli Franzone et al. [4]. All of these models describe the electrophysiology of the cardiac tissue by a reaction-diffusion system of partial differential equations (PDEs) coupled with a system of ordinary differential

equations (ODEs) for the ionic currents associated with the reaction terms.

Bidomain model (B). In this model, intra- and extra-cellular electric potentials $u_i(\mathbf{x},t), u_e(\mathbf{x},t)$ enter into the semilinear parabolic system of two PDEs, while ionic gating variables $w(\mathbf{x},t)$ and ion concentrations $c(\mathbf{x},t)$ arise in the ODE system. Let Ω denote the spatial domain and let the time vary between 0 and T. With the additional notation $v(\mathbf{x},t) = u_i(\mathbf{x},t) - u_e(\mathbf{x},t)$ for the transmembrane potential, the so-called anisotropic bidomain model reads

$$\begin{aligned} c_m\partial_t v - \operatorname{div}(D_i\nabla u_i) + I_{ion}(v,w,c) &= 0 && \text{in } \Omega\times(0,T)\\ -c_m\partial_t v - \operatorname{div}(D_e\nabla u_e) - I_{ion}(v,w,c) &= -I^e_{app} && \text{in } \Omega\times(0,T)\\ \partial_t w - R(v,w) = 0, \quad \partial_t c - S(v,w,c) &= 0 && \text{in } \Omega\times(0,T) \end{aligned} \tag{1}$$

Of course, suitable boundary and initial conditions have to be added. Particular models specify the reaction term I_{ion} and the functions $R(v,w)$ and $S(v,w,c)$.

Monodomain model (M). If an equal anisotropy ratio of the inner- and extracellular media is assumed, then the bidomain system reduces to the monodomain model. This model consists of a single parabolic reaction-diffusion equation for v with the conductivity tensor $D_m = D_e D^{-1} D_i$, $I^m_{app} = -I^e_{app}\sigma^i_l/(\sigma^e_l+\sigma^i_l)$, coupled with the same gating system as above so that we arrive at

$$\begin{aligned} c_m\partial_t v - \operatorname{div}(D_m\nabla v) + I_{ion}(v,w,c) &= I^m_{app} && \text{in } \Omega\times(0,T)\\ \partial_t w - R(v,w) = 0, \quad \partial_t c - S(v,w,c) &= 0 && \text{in } \Omega\times(0,T) \end{aligned} \tag{2}$$

Both the bidomain and the monodomain models have to be completed by membrane models for ionic currents. Since we focus on the Aliev-Panfilov model, we will leave out the more complex Luo-Rudy phase I models (LR1), which can be found in detail in [4].

A FitzHugh-Nagumo model (FHN). The simplest and most popular membrane model is the classical one due to FitzHugh-Nagumo which, however, yields only a rather coarse approximation of a typical cardiac action potential, particularly in the plateau and repolarization phases. A better

approximation is given by the following variant due to ROGERS AND MCCULLOCH [9]:

$$\begin{aligned} I_{ion}(v,w) &= Gv\left(1-\frac{v}{v_{th}}\right)\left(1-\frac{v}{v_p}\right)+\eta_1 vw, \\ \partial_t w &= \eta_2\left(\frac{v}{v_p}-\eta_3 w\right), \end{aligned}$$

where $G, \eta_1, \eta_2, \eta_3$ are positive real coefficients, v_{th} is a threshold potential and v_p the peak potential.

Aliev and Panfilov model (AP). In the present paper, we focus on the suggestion due to ALIEV AND PANFILOV [3], especially designed to model arrhythmia like atrial or ventricular fibrillation. This model is similar to the one of FitzHugh-Nagumo. It describes the relationship between membrane potential v and a recovery variable w. In the frame of the monodomain model, it has the following structure:

$$\partial_t v - \frac{1}{\chi}\Delta v = -I_{ion}(v,w) - I_{st}\,, \tag{3}$$

$$\partial_t w = R(v,w)\,. \tag{4}$$

In our computations, we have used $\chi = 1000.0$. The stimulus I_{st} is an ionic current, applied only for a short time of approximately 1 ms. It starts from a small patch of the heart (e.g., the sinu-atrial node or the atrio-ventricular node). In our simulations, we set $I_{st} = -100$. The original model is dimensionless, but here we have scaled it to obtain physiologically interpretable values. For the ionic current in the membrane I_{ion} we have

$$I_{ion}(v,w) = -(v_p - v_R)(G_A v(v-a)(v-1) + vw)$$

The recovery variable is governed by

$$R(v,w) = 0.25\ (\varepsilon_1 + \mu_1 \frac{w}{v+\mu_2})(-w - G_s v(v-a-1))$$

with $v_p = 35.0$, $v_R = -85.0$, $a = 0.10$, $\varepsilon_1 = 0.01$, $\mu_1 = 0.07$, $\mu_2 = 0.3$, $G_A = 8.0$ and $G_S = 8.0$.

Model complexity. In principle, one would like to use the most complex model, which is the bidomain model coupled with the Aliev-Panfilov model (B-AP), to study fibrillation phenomena. However, the corresponding simulations appear to be extremely expensive. A rough comparison of computational complexity of the various cardiac models is given in Table 1. We present scaled complexity factors estimated from extensive test computations with KARDOS. The factors compare the amount of computational resources (computing time, storage) necessary to solve these problems. They were measured via computations during the regular depolarization phase (first 2 ms after activation) on a small slab of heart tissue, i.e. on the simple geometry as in the recent paper [4].

	domain	membrane model	PDEs	ODEs	Complexity
B-LR1	bi	Luo-Rudy	2	7	200
B-FHN	bi	FitzHugh-Nagumo	2	1	3
M-LR1	mono	Luo-Rudy	1	7	60
M-FHN	mono	FitzHugh-Nagumo	1	1	1
M-AP	mono	Aliev-Panfilov	1	1	1

Table 1: Comparative computational complexity of cardiac models.

2 Simulation Results

In this section, we present the results of our numerical simulations as obtained by the code KARDOS [5, 2]. This code realizes an *adaptive Rothe method*, i.e. a discretization first in time, then in space. In time, it uses a linearly implicit Rosenbrock discretization with stepsize control; in space, it applies an adaptive multilevel finite element method. The estimated errors in time and space are kept below tolerances TOL_t and TOL_x, respectively, to be prescribed by the user. For time integration, we apply the Rosenbrock code ROS3PL as lately developed by Lang [7] (4-stage, third-order, L-stable, no order reduction in the PDE case). Our simulations were performed on the Auckland heart 3D geometry [8]. The associated tetrahedral mesh consists of about 11,306 vertices and 56,581 tetrahedra. In the course of our adaptive refinement, we obtain meshes up to five times locally refined caused by the spatial accuracy requirements (parameter TOL_x). Our finest intermediate meshes have up to 2,100,000 vertices. The arising large sparse linear finite element systems are solved by the iterative solver BI-CGSTAB [12] with

ILU–preconditioning.

First, we present simulation results for accuracy parameters $TOL_t = 0.001$ and $TOL_x = 0.01$. Figures 1, 2, and 3 illustrate the propagation of the front through the heart: After an initial activation (identical to the beginning of the regular heart beat) there is a second activation between 225 and 226 ms, which spoils the build-up of a recovery phase for the whole heart and initiates a chaotic pattern corresponding to ventricular fibrillation. In Figure 4, the effect of spatial adaptivity is illustrated by adaptive meshes in the regular phase (time 70 ms) and the irregular phase (time 580 ms). In Figure 5, temporal adaptivity is exemplified by showing the behavior of the potential v at spatial point $(-3.50, 0.203, 0.174)$. The automatically selected time steps are marked. The computation for time 800 ms was performed on a SUN Galaxy 4600 8 Dualcore AMD and took about 30 GB of memory and about six weeks (!) of CPU time.

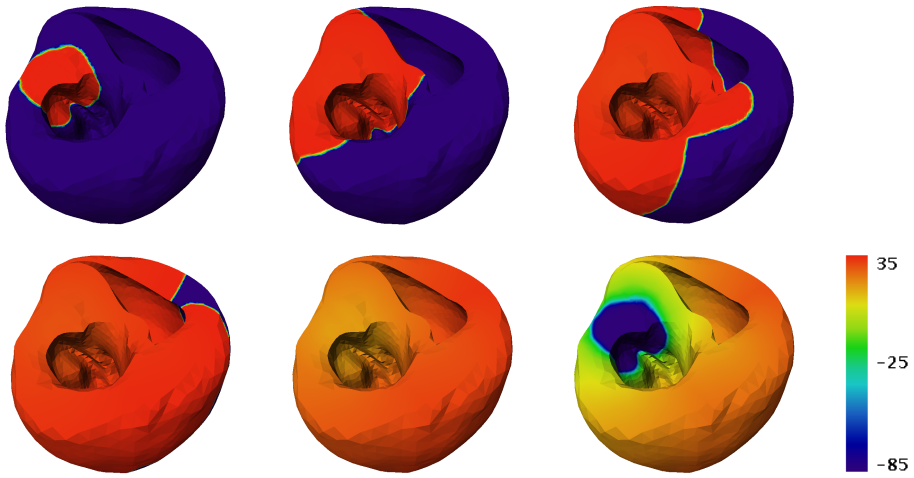

Figure 1: Regular heart beat phase before second activation: potential v at times $10, 40, 70, 100, 160$, and 210 ms (row by row).

Finally, we study the influence of spatial and temporal accuracy requirements on the velocity of the front in the first depolarization phase. In Figure 6, we select the potential v at point $(0.648, 0.521, 1.00)$. The dependence on TOL_x (Figure 6, left) clearly shows that the coarser grid solutions exhibit oscillations before the front and are therefore not acceptable for medical interpretation, whereas the spatially more accurate computations circumvent this shortcoming. The clear message from this finding is that a rather high

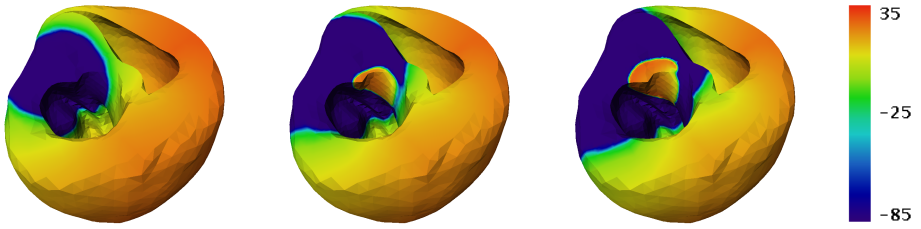

Figure 2: Second activation phase: potential v at times 220, 230, and 240 ms.

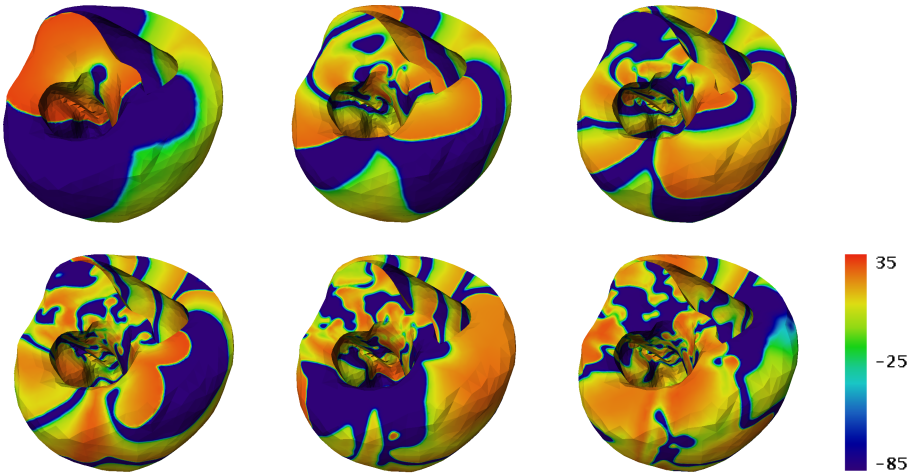

Figure 3: Fibrillation dynamics after second activation: potential v at times $280, 460, 580, 700, 760$, and 820 ms (row by row).

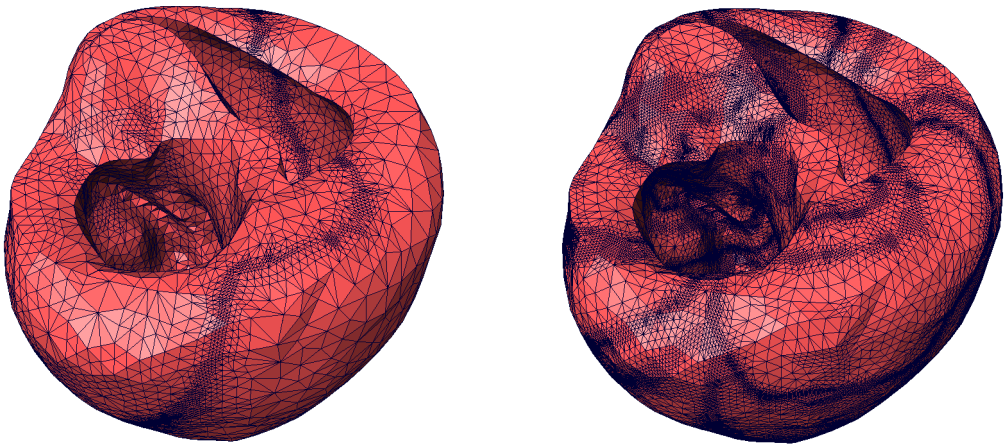

Figure 4: Adaptive meshes. *Left:* Regular heart dynamics at 70 ms. *Right:* Arrhythmic heart dynamics at 580 ms.

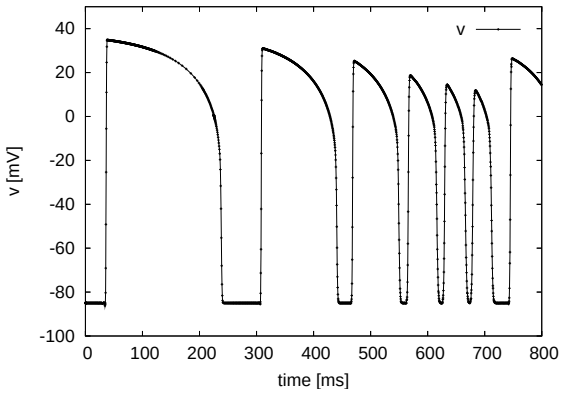

Figure 5: Effect of stepsize control: potential v at point $(-3.50, 0.203, 0.174)$.

accuracy is necessary to approximate the wave front velocity in a reliable manner. In contrast, the dependence on TOL_t (Figure 6, right) turns out to be negligible. The stepsizes corresponding to these accuracy requirements came out as 0.56 ms (for $TOL_t = 0.005$), 0.42 ms (for $TOL_t = 0.002$), 0.33 ms (for $TOL_t = 0.001$), 0.26 ms (for $TOL_t = 0.0005$), and 0.19 ms (for $TOL_t = 0.0002$). On this basis, the choice of $TOL_t = 0.001$ for our computations up to 800 ms seems to be reasonable. For the sake of clarity, we want to mention that these rather big step sizes are a benefit of the new third-order L-stable Rosenbrock integrator.

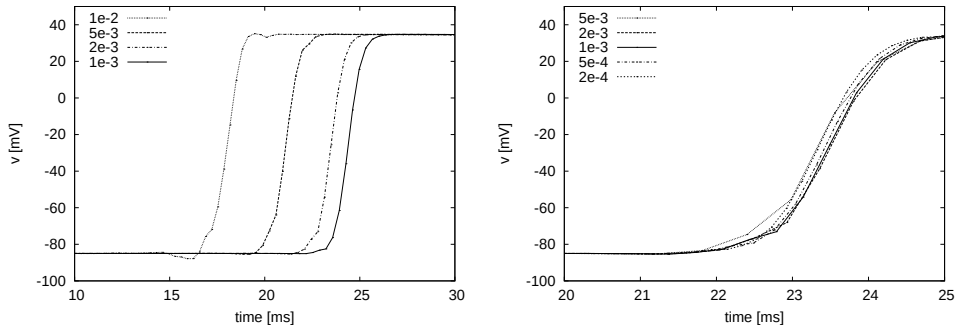

Figure 6: Potential wave front at point $(-3.50, 0.203, 0.174)$. *Left:* Results for different spatial accuracies TOL_x and fixed $TOL_t = 0.001$. *Right:* Results for different temporal accuracies TOL_t and fixed $TOL_x = 0.002$.

Conclusion

In this paper, we applied an adaptive Rothe method (code KARDOS) to study the multiscale fibrillation dynamics within the Aliev-Panfilov cardiac model. Even though this model is rather simple and the algorithm is fully adaptive in both time and space, it requires an amount of computational resources far away from any real-time simulation. The far aim, far away from our present possibilities, is to solve the bidomain Luo-Rudy model for patient-specific 3D heart geometries. Therefore, future work will have to focus on further improvements of the underlying algorithm and its implementation.

Acknowledgements. The authors want to thank Jens Lang, TU Darmstadt, the original main developer of KARDOS, who provided us with a lot

of valuable hints concerning his code. Moreover, we are grateful to Luca Pavarino, University of Milano, for fruitful discussions about electrocardiology models and their simulation.

References

[1] *http://amira.zib.de/*.

[2] *http://www.zib.de/Numerik/numsoft/kardos*.

[3] R. R. Aliev and A. V. Panfilov, *A simple two-variable model of cardiac excitation*, Chaos, Solitons and Fractals, 7 (1996), pp. 293–301.

[4] P. Colli Franzone, P. Deuflhard, B. Erdmann, J. Lang, and L. F. Pavarino, *Adaptivity in space and time for reaction-diffusion systems in electrocardiology*, SIAM J. Sc. Comp., 28 (2006), pp. 942–962.

[5] B. Erdmann, J. Lang, and R. Roitzsch, *Kardos user's guide*, ZIB Report ZR-02-42, Zuse Institute Berlin (ZIB), 2002.

[6] J. Lang, *Adaptive Multilevel Solution of Nonlinear Parabolic PDE Systems. Theory, Algorithm, and Applications*, vol. 16 of LNCSE, Springer-Verlag, 2000.

[7] ——, *ROS3PL - a third-order stiffly accurate Rosenbrock solver designed for partial differential algebraic equations of index one*. Private communication, 2006.

[8] I. LeGrice, P. Hunter, A. Young, and B. Smaill, *The architecture of the heart: a data-based model*, Phil. Trans. Roy. Soc., 359 (2001), pp. 1217–1232.

[9] J. M. Rogers and A. D. McCulloch, *A collocation-galerkin finite element model of cardiac action potential propagation*, IEEE Trans. Biomed. Eng., 41 (1994), pp. 743–757.

[10] D. Stalling, M. Westerhoff, and H.-C. Hege, *Amira: A highly interactive system for visual data analysis*, in The Visualization Handbook, C. Hansen and C. Johnson, eds., Elsevier, 2005, ch. 38, pp. 749–767.

[11] J. Sundnes, G. T. Lines, X. Cai, B. F. Nielsen, K.-A. Mardal, and A. Tveito, *Computing the Electrical Activity in the Heart*, vol. 1 of Monographs in Computational Science and Engineering, Springer, 2006.

[12] H. A. van der Vorst, *BI–CGSTAB: A fast and smoothly converging variant of BI–CG for the solution of nonsymmetric linear systems*, SIAM J. Sci. Stat., 13 (1992), pp. 631–644.